

## Concept for an interferometric test of Hogan's quantum geometry hypothesis

R. Weiss 2/10/2009

**Summary:** The note describes a possible experiment to test the Hogan hypothesis. The concept is to measure the correlations in the optical phase fluctuations at the antisymmetric ports of two Michelson interferometers placed next to each other. The correlation is expected to extend to frequencies as high as  $c/2L$  where  $L$  is the interferometer arm length and  $c$  the velocity of light. For 40 meter arms the correlation spectrum extends to 3.5MHz. Hogan is currently estimating how the correlation falls off with separation of the interferometer beam splitters. The expectation is that the correlation is strong within distances a decent fraction of  $L$ .

Initial estimates using a power recycled Michelson configuration with 1000 watts on the beam splitter (a reasonable value for optics with loss of 100ppm and an input power of 0.5Watt) give an observation time of minutes to achieve unity signal to noise of the Hogan phase fluctuations against the phase fluctuations due to the Poisson noise of the light. The cross correlation of the interferometer outputs is done at frequencies larger than 10kHz where the stochastic forces (displacement and angular thermal noise in mirrors and coatings, seismic and acoustic noise) is negligible relative to the intrinsic photon phase and amplitude noise.

Correlated noise can arise from fluctuations in residual gas density, from scattering if the interferometers share the same vacuum envelope. and simply RF pickup in the electronics. The concept uses separate vacuum systems and separate light sources for the two interferometers. One still needs to take care in avoiding light from one interferometer from entering the other and to avoid common excitation of scattering such as due to high frequency acoustic noise on the interferometer tubes and optics. RF pickup is reduced by careful shielded electronics design.

**Introduction** The experiment is based on the idea that the Hogan quantum geometric phase fluctuations at the output of the two neighboring interferometers are correlated and that an independent sample of the Hogan fluctuation is obtained every  $2L/c$  seconds. The cross correlation of the phase fluctuations due to the correlated Hogan fluctuations will remain as the noise in the cross-correlation from phase noise sources that are uncorrelated is reduced by the square root of the number of independent samples of the cross correlation.

The Hogan angle fluctuations after a round trip of  $2L$  from the beam splitter are

$\delta\theta_{\text{Hogan}} = \sqrt{\frac{\lambda_{\text{Planck}}}{L}}$  with  $\lambda_{\text{Planck}} = 1.6 \times 10^{-33}$ , the Planck length. The inferred displacement is

$\delta x_{\text{Hogan}} = \sqrt{L\lambda_{\text{Planck}}}$  which becomes an alarmingly large number for a 40 meter arm length of  $2.5 \times 10^{-15}$  cm. The optical phase shift at the antisymmetric port associated with this displacement

is  $\delta\phi_{\text{Hogan}} = \frac{2\pi\delta x_{\text{Hogan}}}{\lambda_{\text{opt}}}$ . The Hogan optical phase spectral density for a 40 meter arm becomes

$\phi(f) = 8 \times 10^{-14}$  radians/ $\sqrt{\text{Hz}}$  with a flat spectrum between DC and 3.5MHz.

The phase at the individual interferometer outputs is

$$\begin{aligned}\phi_1 &= \phi_{n1} + \phi_{\text{Hogan}} \\ \phi_2 &= \phi_{n2} + \phi_{\text{Hogan}}\end{aligned}$$

The cross correlation at zero delay averaged over N samples is approximated by (the cross term between the correlated and uncorrelated terms is neglected)

$$(\phi_1 X \phi_2)_N = \frac{(\delta\phi_n)^2}{\sqrt{\frac{t_{\text{obs}}}{\tau_{\text{sample}}}}} + (\delta\phi_{\text{Hogan}})^2$$

where it is assumed that the independent phase noise in the two interferometers has the same vari-

ance.  $N = \frac{t_{\text{obs}}}{\tau_{\text{sample}}}$  is the total number of samples in the measurement.

An estimate for the observation time required to have the correlated variances be equal to the uncorrelated one is when the two terms in the cross correlation become equal

$$t_{\text{obs}} > \tau_{\text{sample}} \left( \frac{(\delta\phi_n)^2}{(\delta\phi_{\text{Hogan}})^2} \right)^2$$

If the dominant independent noise comes from intrinsic quantum phase fluctuations of the light (the Glauber state for the electromagnetic field of the laser which has a Poisson distribution in photon number), the variance in the phase in a sample  $2L/c$  long is

$$(\delta\phi_n)^2 = \frac{1}{n} = \frac{1}{\dot{n} \tau_{\text{sample}}} = \frac{hc^2}{2P_{\text{BS}} L \lambda_{\text{opt}}}$$

where  $P_{\text{BS}}$  is the optical power at the symmetric port of the beam splitter and  $\lambda_{\text{opt}}$  is the wave length of the light. The expression for the unity signal to noise observation time becomes

$$t_{\text{obs}} > \left( \frac{h}{P_{\text{BS}}} \right)^2 \left( \frac{\lambda_{\text{opt}}}{\lambda_{\text{pl}}} \right)^2 \left( \frac{c^3}{32\pi^4 L^3} \right)$$

The proposed parameters for the concept experiment:  $L = 4 \times 10^3$  cm,  $\lambda_{\text{opt}} = 1.06 \times 10^{-4}$  cm and  $P_{\text{BS}} = 1000$  watts. The Poisson optical phase noise becomes  $\phi(f) = 1.3 \times 10^{-11}$  radians/ $\sqrt{\text{Hz}}$  about 150 times larger than the Hogan noise amplitude spectrum. The observation time to a signal to noise of unity needs to be longer than 3.5 minutes, approximately 1/2 hour is needed to achieve a 3 sigma result in the Hogan noise power.

**Interferometer model:** The proposed instruments are power recycled Michelson interferometers using optics with loss of 100ppm for the beam splitter and the two end mirrors and with a coating loss less than 100ppm for the recycling mirror. The power entering the interferometer at the recycling mirror is 0.5 watts. The laser frequency tracks the fluctuations in common mode arm length  $((L_x + L_y)/2)$  by frequency control of the laser through a Pound, Drever, Hall reflection locking system at the recycling mirror. The differential length  $((L_x - L_y)/2)$  is maintained to hold the light

at the antisymmetric port to a desired DC offset by PZT drivers on the end mirrors. The fringe interrogation uses slope detection of the fringe (a DC readout) but with a bandwidth extending to 10 MHz. The range of the PZT controllers is determined by the amount of thermal expansion drift and low frequency seismic noise that needs to be removed to hold the differential output of the interferometer to stay locked on a single fringe. The required range needs to be measured in the experiment location but is most likely smaller than several microns with reasonable laboratory temperature control and typical building low frequency seismic noise. A schematic of the interferometer is shown in **Figure 1**.

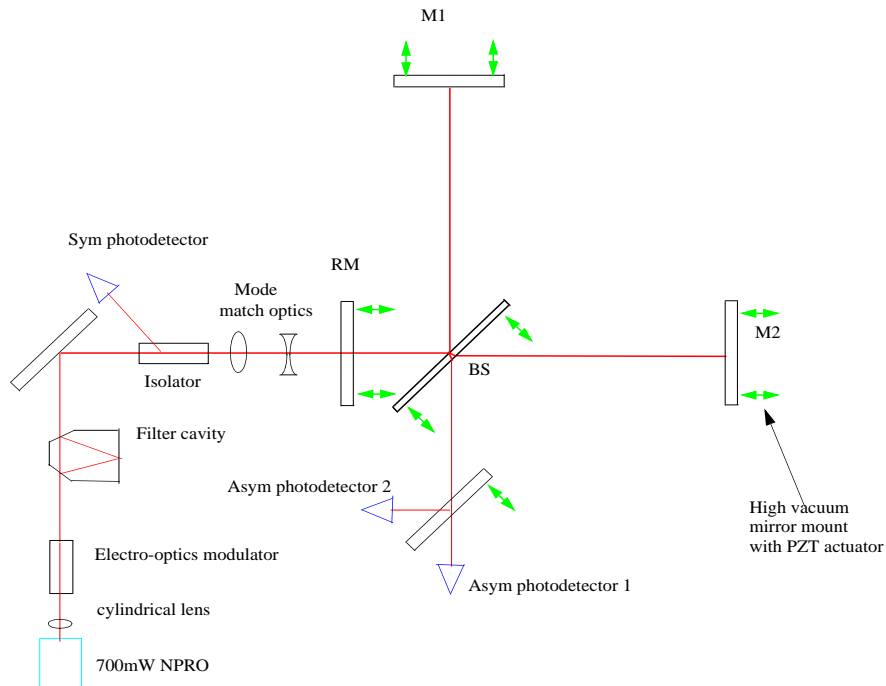


**Figure 1** Schematic of the proposed optical configuration. An important question is to determine which of the optical elements need to be in the vacuum. Initially the end mirrors, beam splitter and recycling mirror and the paths between them need to be in vacuum. It may well turn out that unexpected correlations will require the antisymmetric optics and photodetectors to be in the vacuum as well. It would be prudent to plan a single chamber that could hold the RM, BS and the asymmetric port optics and photodetectors, although initially one could try the experiment with the antisymmetric port optics and photodetectors on the outside using a high quality optical window. It may not be necessary to include the filter cavity in the optical train. The cavity is intended to remove the relaxation oscillations of the laser which occur between 50 to 70kHz from the optical beam. We need to look at the amount of amplitude filtering that will come from the recycling process itself. Several manufacturers now sell high vacuum worthy mirror mounts with PZT controllers.

## Relations from the interferometer model

The results of scattering matrix model of the interferometer are shown in **Figure 2** through **5**. The power hitting the symmetric port of the beam splitter as a function of the amount of power leaving the antisymmetric port due to an offset between the two arms is shown in **Figure 2**.

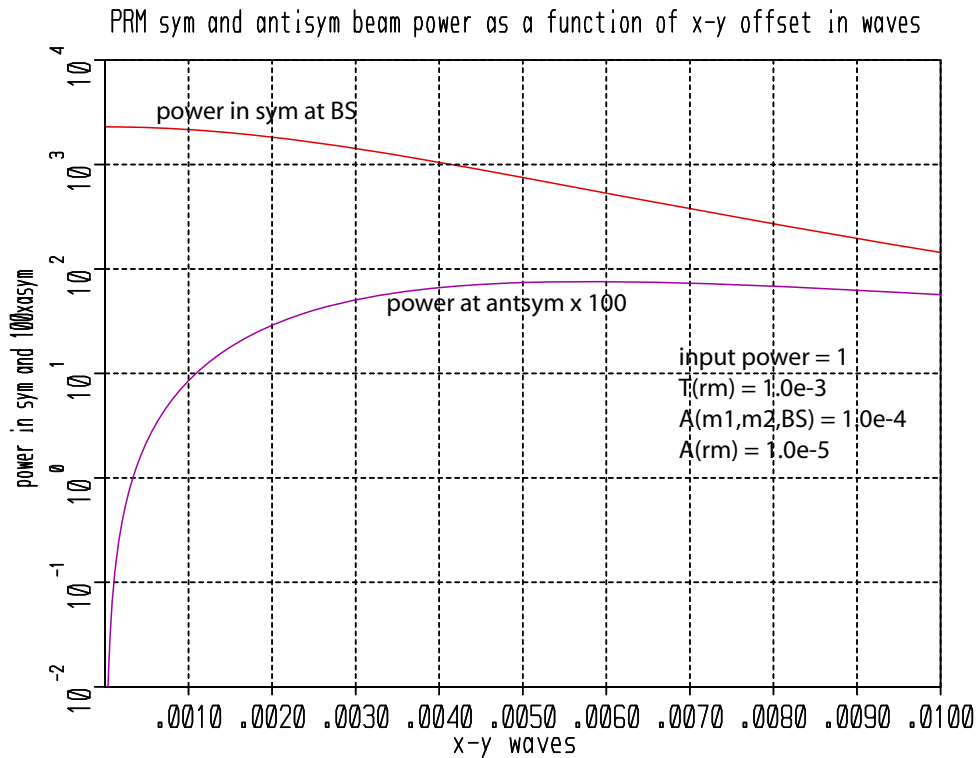


**Figure 2** The transmission of the recycling is optimized when it is equal to the sum of the mirror loss  $A$  plus the ratio of the power emitted at the antisymmetric port to the power at the symmetric port. The recycling power gain could be closer to  $1/A$  with a smaller recycling mirror transmission but the system becomes more difficult to work with. The change in power at the antisymmetric photodetector with phase difference between the arms is  $\frac{dP_{\text{detector}}}{d\phi} = \frac{2P_{\text{in}}\phi_{\text{offset}}}{A}$  for small offsets (less than  $5 \times 10^{-3}$  waves). The DC photo current depends on the  $(\phi_{\text{offset}})^2$  for small offsets. As a consequence, the phase sensitivity, the ratio of the  $\frac{dP_{\text{detector}}}{d\phi}$  to the shot noise at the detector, is independent of the offset for small values. The phase sensitivity is close to the value used in estimating the observing time. The amount of differential offset needed depends on several experiment parameters to be estimated later in this note.

The power at the antisymmetric port is (exact expression)

$$\frac{P_{\text{antisym}}}{P_{\text{in}}} = \frac{T_{\text{rm}} R_{\text{bs}} T_{\text{bs}} [R_{\text{m1}} + R_{\text{m2}} - 2\sqrt{R_{\text{m1}} R_{\text{m2}}} \cos(2k\Delta x_{1,2})]}{1 + R_{\text{rm}} [T_{\text{bs}}^2 R_{\text{m2}} + R_{\text{bs}}^2 R_{\text{m1}} + 2R_{\text{bs}} T_{\text{bs}} \sqrt{R_{\text{m1}} R_{\text{m2}}} \cos(2k\Delta x_{1,2})] - 2\sqrt{R_{\text{rm}}} [\chi]}$$

$$\chi = T_{\text{bs}} \sqrt{R_{\text{m2}}} \cos(2k\Delta x_{\text{rm},2}) + R_{\text{bs}} \sqrt{R_{\text{m1}}} \cos(2k\Delta x_{\text{rm},1})$$

A streamlined approximate expression is given below providing : losses in rm1 and rm2 = A , the beam splitter is truly a 50/50 device with negligible loss, the resonance condition for the power recycling is obtained in the common mode spacing of the mirrors and the recycling mirror loss can be neglected.

$$\frac{P_{\text{antisym}}}{P_{\text{in}}} = \frac{T_{\text{rm}} (1 - A) [1 - \cos(2k\Delta x_{1,2})]}{2[1 - \sqrt{(1 - T_{\text{rm}})(1 - A)} \cos(2k\Delta x_{1,2})]^2}$$

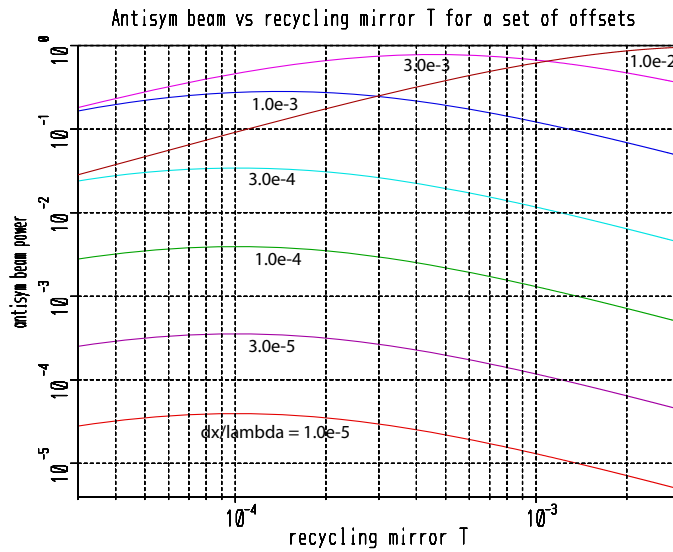


**Figure 3** Power at the antisymmetric port for an interferometer with mirror loss  $10^{-4}$  as a function of the recycling mirror transmission and for a variety of differential offsets. The recycling mirror transmission is optimized close to the mirror loss.

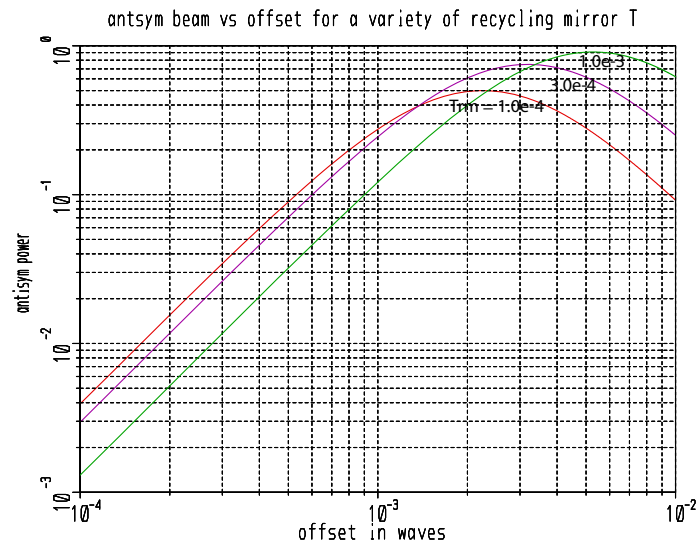


**Figure 4** Antisym output power vs differential offset in waves for three recycling mirror transmissions,  $T$ .

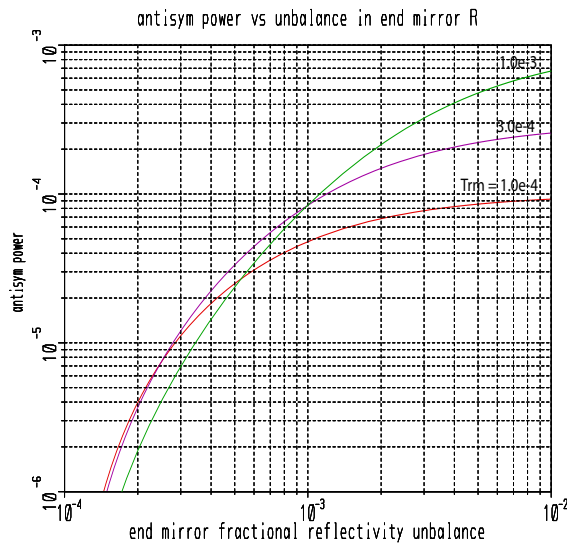


**Figure 5** Antisym output power as a function of fractional reflectivity unbalance between M1 and M2. This unbalance along with mirror figure error and the relative irreducible rms motion of the arm lengths determines the contrast defect of the interferometer - the power at the antisymmetric output even with nominally equal interferometer arms. This unmodulated light adds to the shot noise budget without giving increased sensitivity for the interferometer phase.

**Preliminary estimates for the optics** A first try at the design has the recycling mirror and the two end mirrors with the same radius of curvature while the beam splitter is flat. Since one would hope to use available low loss mirrors it is worthwhile being flexible in the cavity design as it does not seem that there is a particular difficulty with the mode structure of the recycling cavity

except to stay away from known geometric instabilities. A symmetric cavity with the beam waist at  $\sim 20$  meters is chosen. The g factor used for all the mirrors is 0.45 yielding a mirror radius of 22

meters. The Gaussian beam ( $1/e^2$ ) waist radius given by  $\sqrt{\frac{L\lambda_{opt}}{\pi}}$  is 3.67 mm while the beam radius at the mirrors is  $w = 3.95$  mm. One inch diameter mirrors ( $r_{mirror}$ ) at the ends and for the

recycling would give a diffraction loss  $e^{-2\left(\frac{r_{mirror}}{w}\right)^2} = 1 \times 10^{-9}$ .

## **The noise sources (Note this section will continue to be iterated)**

### **1) Thermal noise in the photodetector load resistor and preamplifier noise**

Assume that we will be using RF components standard 50 ohm terminations. The thermal noise current generated by a 50 ohm resistor at 300K is  $2 \times 10^{-11}$  amp/ $\sqrt{\text{Hz}}$  and decent amplifier input noise is  $1 \times 10^{-9}$  V/ $\sqrt{\text{Hz}}$ . The Poisson noise of the modulated light should exceed these values by at least a factor 3. The photocurrent that can be modulated needs to be 3 milliamperes or larger. With InGaAS photodiodes that have a quantum efficiency of 0.8, the power hitting the photodetector should then be about 4 milliwatts/photodiode. With two photodiodes the antisymmetric power needs to be 8 milliwatts. With 1/2 watt input power at the recycling mirror, the ratio of the power at the antisymmetric port to the input power (the quantity used in the figures) is then  $1.6 \times 10^{-2}$ . Using Figure 4, the fringe offset required is about  $3.5 \times 10^{-4}$  waves.

### **2) Additional Poisson noise due to poor fringe contrast**

Estimates for the unmodulated light at the antisymmetric port :

a) Unbalance in the reflectivity of M1 and M2 . The power at the antisymmetric output is second order dependent on the fractional difference in reflectivities of M1 and M2. The antisymmetric

power varies as  $\frac{P_{in}(\Delta R)^2}{2A}$ . It would good, but not essential, to match the reflectivities to  $2 \times 10^{-3}$

b) rms relative motion of the mirrors M1 and M2. The relative motion of the two end mirrors is best not much larger than the fringe offset determined by the amplifier noise. If one allows the relative motion to be equal to the offset, it corresponds to about  $3 \times 10^{-7}$  cm rms motion. If the relative vibrational noise in the space is 3 microns rms with most of the energy at 10 Hz and smaller, the forward loop gain of the fringe control signal needs to be about  $10^4$  with a bandwidth of at least 10kHz. The design of this servo with appropriate PZT controllers is one of main design tasks for the experiment once the vibration has been measured. There may well be resonances in the structure which will require special filtering in the control system. There may also be pleasant cancellations due to common mode motion in the building. All this argues for a digital control system with the simplicity of digital filtering to hold the fringe but not to interrogate it, that could remain analog.

### 3) Equivalent phase noise from amplitude fluctuations

The excess amplitude noise in the light above the Poisson fluctuations needs to be controlled to a level equal or below the Poisson noise. The Poisson fluctuations of the 4 milliamperes per photodiode corresponds to a relative intensity noise of  $9 \times 10^{-9}$ . The Hogan signal band will be above 10kHz so that the standard noise sources due to vibration and cooling will not be important. The relative intensity noise of the commercial NPRO was measured at LIGO and also in Hanover. At frequencies above 10kHz one can achieve  $10^{-7}$  with pump stabilization and  $8 \times 10^{-9}$  with photodiode stabilization using electro-optic amplitude modulators. Alternatively or in addition one can use an optical filter cavity which helps in reducing the amplitude noise due to the relaxation oscillations. High frequency amplitude noise does need to be tended to in this experiment, especially if there is too much unmodulated light at the antisymmetric port.

### 4) Direct phase noise from frequency noise

The principal means for laser frequency fluctuations to cause phase noise in the interferometer is through path length difference between the two arms. In a Michelson interferometer it is reasonably easy to find the operating point that greatly reduces this source of phase noise. One executes a search for the “white” light fringe, the fringe that minimizes the modulation measured from a frequency modulated light source. The NPRO lasers have around  $v(f) = 10^{-2} \text{ Hz}/\sqrt{\text{Hz}}$  frequency noise above 10kHz when free running. The frequency noise sensitivity of the measurement is

given by  $\phi(f) = \frac{2\pi v(f)\Delta x}{c}$ , where  $\Delta x$  is the path length difference. The phase noise should be

less than the Poisson driven phase noise given previously which requires the path length difference be less than 6 cm.

### 5) Phase noise from scattering paths coupled through frequency fluctuations

The scattering paths will involve a scatter from a mirror then a reflection or another scattering by the wall and ultimately recombination with the main beam on a mirror. We studied this process for LIGO in a model where the ground noise and acoustic excitation of the scattering surfaces were the primary phase modulators. (The mirrors are suspended and not themselves modulators, they are sources and recombiners of the scattered light.) In LIGO we did baffle the tubes to avoid multiple bounce paths from mirror to mirror. At the frequencies involved in this Hogan search the acoustic and seismic motions will not have components in the fringe interrogation band and even the worst case fringe wrapping motions are not expected to up-convert 10's of Hz into the region above 10kHz. The primary source of phase noise from scattering will come from the scattered paths having taken different times than the main beam before recombination. The phase noise would then come from the frequency noise of the light source being sampled at different times by the scattered beams before recombination with the main beam. The effect would be similar to the path length unbalance formulation above but with the ratio of the scattered field to the main field as an additional multiplying factor. The phase noise would symbolically be

$$\phi(f) = \frac{2\pi v(f)}{c} \sum_i \left[ \frac{E_i \Delta x_i}{E_{\text{main}}} \right]$$
 although this is a vector sum. A quick guess is that longest path

would be  $4 \times 10^3$  cm. Using the same NPRO frequency noise as above would then require that the scattered field to main field ratio be  $10^{-3}$  or smaller, the intensity ratio  $10^{-6}$ . These are not terrible

numbers but, this clearly needs more work. Especially the nature of the baffling and the scattering functions for the mirrors need to be looked at. The LIGO experience is better than this requirement, however, we have found places where the scattered light is close to being specularly reflected where we have had to erect blocks and baffles.

### 6) Phase noise from forward scattering by the residual gas

The fluctuations in the column density of the gas due to the molecular motions causes fluctuations in the phase due to the forward scattering of the residual gas molecules. The scattered field by the molecules when recombined with the main beam causes the phase fluctuations (another way of talking about the index of refraction). The phase fluctuations from statistical mechanics are given by

$$\phi(f) = \frac{8\pi^2 \alpha L^{\frac{1}{4}} \sqrt{\rho}}{\lambda^{\frac{5}{4}} \sqrt{v}} e^{-\frac{f\sqrt{2\pi\lambda L}}{v}}$$

$\rho$  is the particle density in number/cc,  $\alpha$  is the molecular polarizability in cc at the wavelength of the light and  $v$  is the molecular average velocity. The exponential is needed since the distribution of molecules over the beam cannot change faster than the time for an atom to cross the beam. Using  $\alpha = 1.5 \times 10^{-24}$  cc as the polarizability of molecular nitrogen, and  $v = 5 \times 10^4$  cm/sec as the thermal velocity of the molecule, the particle density to have this phase noise be 1/10 of the Poisson phase noise becomes  $1 \times 10^{13}$  molecules/cc or a pressure of about  $10^{-4}$  torr. (I had this number wrong in my original estimate). It would be better to have a lower pressure to avoid mirror contamination.

### Worries and things to consider

Besides the usual worries that one has forgotten something, my chief concern is whether the simple idea of a one dimensional longitudinal control system will be sufficient to hold the fringe well enough. It may also be necessary to adjust for varying pointing angles. The hedge against this is to use vacuum compatible mirror mounts with PZT control on displacement as well as pitch and yaw. So far no automated system to do the alignment is being considered, if it becomes necessary, a dither alignment scheme could be used. A good bit of these concerns would be alleviated if one sets up some mirrors with pointing lasers and quadrant photodiodes to measure angular fluctuations in the space offered to carry out the experiment. This and the measurement of the ground motion by three seismometers placed at the locations of the vertex and ends of the interferometer would be a good first step. The seismometers would be crosscorrelated to establish the differential and common mode parts of the local seismic spectrum.

Another worry is really the RF pickup which can cause correlations between the two interferometers. Clearly, one would do the usual things to shield both the transmitters and the receivers and perform rigorous tests.

### Preliminary budget estimate

The optics and lasers are estimated based on that Fermi lab does not have a good stockpile of 1 micron coated optics or precision optical components. No estimate is made for the vacuum system as it assumed that Fermi would have stuff around and would also have better handle of the costs and availability. General purpose electronics is also not estimated . Here, again it assumed that Fermi has a good collection of RF and analog electronics. A unique electronic instrument would be a correlator or fast digital system to carry out the correlation directly in the digital domain.

**Table 1: Optics estimates**

| number   | item                                       | source                    | cost/item | total cost |
|--|--|---------------------------|-----------|------------|
| 2  | 750 mW NPRO                                | JDSU                      | 29K       | 58K        |
| 8  | InGaAs photodetectors                      | Thor Lab                  | 0.5K      | 4K         |
| 2  | Electro-optic modulator                    | New Focus                 | 3.1K      | 6.2K       |
| 10   | Vacuum compatible PZT driven mirror mounts | New Focus                 | 1.9K      | 19K        |
| 2  | Faraday isolators                          |                           | 3K        | 6K         |
| 4  | optical quality vacuum windows             |                           | 1K        | 4K         |
| 10   | super polish and coated mirrors            | General optics or Newport | 0.5K      | 5K         |
| 2  | filter cavities                            |                           | 15K       | 30K        |
| 4  | optics tables                              | TMC                       | 3K        | 12K        |
| 20   | 1.06 micron coated lenses                  | Newport                   | 0.1K      | 2K         |
| Total  |  |                           |           | 146K       |
| 1  | superpolishing run                         |                           | 10K       | 10K        |
| 3  | coating run                                |                           | 10K       | 30K        |
| Total with runs but no superpolished generic mirrors |  |                           |           | 181K       |

There may well be merit in having mirrors polished and coated specifically for this experiment. This option is the reason for the second estimate.